Acquisition and voxelwise analysis of multi-subject diffusion data with Tract-Based Spatial Statistics

Stephen M Smith[1], Heidi Johansen-Berg[1], Mark Jenkinson[1], Daniel Rueckert[2], Thomas E Nichols[1,3], Karla L Miller[1], Matthew D Robson[4], Derek K Jones[5], Johannes C Klein[1], Andreas J Bartsch[6] & Timothy E J Behrens[1]

[1]Oxford University Centre for Functional Magnetic Resonance Imaging of the Brain (FMRIB), Oxford, UK. [2]Department of Computing, Imperial College London, London, UK. [3]GlaxoSmithKline Clinical Imaging Centre, London, UK. [4]Department of Cardiovascular Medicine, Oxford Centre for Clinical Magnetic Resonance Research, Oxford, UK. [5]Cardiff University Brain and Repair Imaging Centre, Cardiff, UK. [6]Department of Neuroradiology, University of Wuerzburg, Wuerzburg, Germany. Correspondence should be addressed to S.M.S. (steve@fmrib.ox.ac.uk).

Published online 15 March; corrected online 29 March 2007 (details online); doi:10.1038/nprot.2007.45

There is much interest in using magnetic resonance diffusion imaging to provide information on anatomical connectivity in the brain by measuring the diffusion of water in white matter tracts. Among the measures, the most commonly derived from diffusion data is fractional anisotropy (FA), which quantifies local tract directionality and integrity. Many multi-subject imaging studies are using FA images to localize brain changes related to development, degeneration and disease. In a recent paper, we presented a new approach, tract-based spatial statistics (TBSS), which aims to solve crucial issues of cross-subject data alignment, allowing localized cross-subject statistical analysis. This works by transforming the data from the centers of the tracts that are consistent across a study's subjects into a common space. In this protocol, we describe the MRI data acquisition and analysis protocols required for TBSS studies of localized change in brain connectivity across multiple subjects.

INTRODUCTION

The diffusion of water in brain tissue is affected by the local tissue microstructure; for example, water diffuses more easily along the major axis of a white matter fiber bundle than it does perpendicular to it[1]. Magnetic resonance diffusion tensor imaging (DTI) is sensitive to water diffusion characteristics and has been developed as a tool for investigating the local properties of brain tissues such as white matter tracts[2]. There has been great interest in using diffusion anisotropy as a marker for white matter tract integrity, for example for disease diagnosis, tracking disease progression, finding disease subcategories, studying normal development or aging and as complementary information to functional magnetic resonance imaging (FMRI) for investigating brain function[3–6]. Further relevant background or reference material includes diffusion MRI physics[7] and a white matter brain atlas[8].

Diffusion anisotropy exists in systems where water diffusion is hindered more in some directions than in others, and is most simply quantified through a standard measure known as fractional anisotropy (FA)[9]. FA is highest in major white matter tracts (maximum theoretical value 1), lower in gray matter, and approaches 0 in cerebrospinal fluid. Variation in FA in white matter reflects multiple factors, including myelination, axon density, axonal membrane integrity, axon diameter[10] and intravoxel coherence of fiber orientation. As a marker for tract integrity, FA is a useful quantity to compare across subjects, as it is computable voxelwise and is a scalar value that is independent of the local fiber orientation (and is therefore an objective and straightforward measure). Some researchers have simply summarized diffusion characteristics globally (e.g., using histogram-based measures) to compare different subjects. However, most recent work has focused on spatially localizing diffusion-related changes.

Some studies have, to this end, used voxelwise analyses based on an initial alignment of the diffusion data to a standard brain image (standard space), spatial smoothing and then voxelwise (localized) cross-subject analysis of the resulting aligned data. Such an analysis is often referred to as voxel-based morphometry (VBM), originally developed for finding local changes in gray matter density in T1-weighted structural brain images[11]. There has been much debate about the limitations of such an approach, primarily because there can be ambiguity as to whether apparent changes are truly due to change in gray matter density or simply due to spatial misalignment. When applied to FA data, this is particularly concerning; how can one guarantee that any given 'standard space' voxel contains data from the same part of the same white matter tract from each and every subject?

The primary advantage of voxelwise analyses (compared, say, with tractography-based analysis) is that the entire brain can easily be investigated in a fully automated manner, without having to specify in advance regions of interest or delineate (normally by hand) which specific tracts to test.

Recently, we proposed an approach to carrying out localized statistical testing of FA (and other diffusion-related) data that aims to alleviate alignment-related problems[12]. We refer to this new approach as tract-based spatial statistics (TBSS). In this approach, FA images of all subjects are first aligned into a standard brain space using non-linear registration[13]. Next, the mean of all subjects' aligned FA images is created, and then 'thinned' using standard image processing techniques to create a mean FA skeleton that represents the centers of major tracts common to the group of subjects. Each subject's aligned FA data is then projected (perpendicular to the local tract direction) onto this skeleton so that the projected FA values are taken from the centers of the tracts in the original FA image. This projection aims to resolve any residual correspondence (alignment) problems after the initial non-linear registration. The resulting data are then fed into voxelwise (localized in the image) cross-subject statistics to identify where, for example, tract integrity has been damaged through disease progression or where, in normals, tract integrity appears to correlate with ability to carry out a given task.

Note that a voxelwise analysis such as TBSS does not directly inform the researcher on long-range structural connectivity in the brain, but is limited to investigating local changes in white matter structure. It should not, therefore, be used as a replacement for careful tractography-based connectivity analysis of diffusion data, which should ideally be used in conjunction with a voxelwise analysis. Note also the possible risk of failure of cross-subject image alignment; gross variations in brain organization caused by stroke lesions or tumors, for example, are likely to invalidate any voxelwise analysis.

Here, we describe the acquisition protocol required to generate diffusion MRI data of sufficient quality to feed into a TBSS analysis. We then describe the analysis protocol, including comments on how to check the different stages of the analysis, statistical inference issues and possible pitfalls.

BOX 1 | DIFFUSION DATA ACQUISITION REQUIREMENTS

ESSENTIAL MINIMUM STANDARDS

- The **field-of-view** should encompass the whole brain.
- The **voxel size** should be less than $3 \times 3 \times 3$ mm^3. If voxels with larger dimensions are acquired, analysis will be possible for only the thickest tracts. Isometric (cubic) voxels are preferred, but not necessarily crucial, for tract-based spatial statistics (TBSS).
- At least one $\boldsymbol{b = 0}$ (no diffusion weighting) image should be acquired; ideally one $b = 0$ image for (approximately) every eight diffusion-weighted images[18].
- A **diffusion-weighting *b*-value** of at least 800 s mm^{-2} is recommended.
- At least six different (non-coplanar) **diffusion gradient directions** must be acquired. Often several repeats of each will be acquired to improve signal-to-noise ratio (SNR). If time permits more than six images to be acquired, it is better to use more unique sampling directions (with isotropic angular density[18]) than to obtain repeat samples of the same set of directions, from the point of view of both tensor fitting[19] and tractography analyses[20].
- **SNR**[21] in the diffusion-weighted images should be maximized, but is difficult to control and quantify directly as it depends on many factors such as the *b*-value, the non-diffusion-weighted SNR and the number of diffusion-weighted averages/directions. An example protocol that should lead to sufficiently high SNR is having $b = 1{,}000$ s mm^{-2}, 24 diffusion-weighted images and SNR greater than 15 in the $b = 0$ image.
- The data should **not be upsampled** (e.g., through unfiltered zero-padding during reconstruction) if this is done in such a way as to introduce ringing into the data.
- If multiple repeats of $b = 0$ or diffusion-weighted images are to be acquired, they must **not be averaged on the scanner** (as they must be co-registered before averaging, and any risk of averaging the complex data should be avoided).
- **Fat saturation** should be used whenever possible to remove signal from the scalp, which can disrupt signal in the brain owing to chemical shift or ghosting artifacts.
- A vitamin capsule **left–right marker** (oil, not water) should be attached to the right side of the head to avoid any left–right ambiguities during data conversion and analysis.

OPTIONAL PROCEDURES

- If multiple repeats of gradient directions are to be acquired, then **varying the phase encoding direction** (often referred to in the simplest cases as 'blip-up, blip-down') across different repeats can allow for distortion correction during reconstruction[22]. Phase encoding (for axial or coronal imaging) should ideally preserve hemispheric symmetry (i.e., should not be left–right), for aesthetic reasons, although successful distortion correction eliminates this restriction.
- The diffusion imaging **pulse sequence** will most likely be single-shot echo-planar imaging (EPI); however, spiral scanning[23] and periodically rotated overlapping parallel lines with enhanced reconstruction (PROPELLER) fast spin echo (FSE)[24] are also used with success. PROPELLER is particularly well suited for subjects with increased risk of head motion during scanning (e.g., very young subjects or patients with movement disorders) but increases the total imaging time.
- To enhance SNR, both **TE** (echo time) and readout **bandwidth** should be minimized; however, these tend to be competing goals (reducing bandwidth may increase TE). The choice of bandwidth also affects the distortions in EPI, where higher bandwidth incurs less distortion. A good strategy is to determine the lowest bandwidth with an acceptable level of distortion for the specified matrix size (e.g., 1,000 Hz per pixel, or 1 ms echo spacing for a 64×64 image matrix) and then to minimize the TE (preferably to below 100 ms).
- **Partial k-space imaging** (e.g., acquiring only a fraction of k-space) can also reduce TE, and therefore increase SNR; however, this increase is typically modulated by the reduction in SNR caused by the reduced total readout duration. As above, these trade-offs are complex[25], but acquiring three-fourths of k-space is often a good choice.
- If the system allows it, the acquisition should be **triggered to avoid the systolic phase of the cardiac cycle**[26]. When ECG chest leads are used, a delay of at least 250 ms after the R-wave should be employed. More conveniently, a peripheral pulse-oximeter placed on a finger of the participant may be used, for which a minimal trigger delay (approximately 20 ms) is sufficient to avoid pulsatility artifacts.
- **Parallel imaging**[27] (which MRI vendors may refer to as SENSE, iPAT, GRAPPA or ASSET) may be used (particularly at higher field strength) to reduce EPI distortion[28]. Parallel imaging has similar SNR trade-offs to partial k-space imaging, with an additional SNR penalty owing to the dependence of reconstruction fidelity on coil geometry. However, TBSS is relatively insensitive to distortions, and thus parallel imaging may not be worthwhile[29]. The acceleration factor should probably be limited to two to minimize reconstruction artifacts.
- **Multiple channel head coils** generally give better SNR than single-channel (e.g., birdcage) coils, although if used in combination with parallel imaging, the SNR gain may decrease.

MATERIALS

REAGENTS

- Subjects ▲ CRITICAL Ensure that the study protocol is approved by the appropriate ethical review board. Ensure that a sufficient number of subjects are included in the study through the use of power calculations. Previous estimates of variation in reproducibility of diffusion measures may be helpful in this regard[12,14]. Different groups of subjects should be carefully matched, at least for age and gender. Data from subjects with gross localized pathology, particularly those with mass lesions or edema, should be used with great caution in this type of analysis. Non-linear registration may be unable to correct for gross structural change, and perifocal edema will strongly influence the measured FA. As lesions tend not to be in the same location across subjects, analysis of group studies will be difficult.

EQUIPMENT

- MRI scanner (see EQUIPMENT SETUP)
- Computing equipment (see EQUIPMENT SETUP)

EQUIPMENT SETUP

MRI scanner with whole-head diffusion MRI capability (see minimum data quality standards in **Box 1**) and with field strength likely to be in the range 1.5–3 T. Signal-to-noise ratio (SNR) is generally better at higher field strength, but distortions are worse. The latest clinical scanners from Siemens, GE and Philips have multiple direction (greater than 6) diffusion capability.

Computing equipment We recommend using Unix-based computers. FMRIB Software Library (FSL) is available in precompiled form for Apple Mac (running Mac OS X version 10.4 or higher) and PCs (running Linux flavors RedHat 9, Enterprise, FC4, Suse 9.0-9.3 or Debian) and is therefore easiest to install with one of these options. As some TBSS programs can have high RAM requirements (particularly if tens of subjects are used in a study), it is likely that the computer will need to be 64 bit. The computer should have at least a 1 GHz CPU clock, 1 GB RAM, 5 GB swap and 20 GB free hard disk space. If multiple networked computers (or a computer cluster) are available, the registration steps can be parallelized, greatly reducing the total computation time. The FSL software package (freely available for non-commercial use at http://www.fmrib.ox.ac.uk/fsl) is the minimum software that needs to be installed on top of a standard Unix-based operating system to carry out a complete TBSS analysis.

PROCEDURE

Obtaining subjects' informed consent ● TIMING 10 min per subject

1| Obtain informed consent from subjects and document relevant characteristics and clinical data as well as handedness.

Acquisition of MRI data ● TIMING 30–60 min per subject

2| Take a high-resolution T1-weighted structural image (recommended). Although this is not currently required for the standard TBSS analysis protocol, there are many other analyses and applications of diffusion data that can benefit from having a structural image to combine with the diffusion data. The acquisition should include the whole brain, with suggested voxel dimensions of $1 \times 1 \times 1$ mm^3. It should be possible to acquire a high-quality structural image easily and quickly on a state-of-the-art clinical scanner, for example, by averaging $3 \times$ 5-min 3D scans.

3| Use exactly the same imaging protocol for all subjects. The diffusion data should meet the minimum standards described in **Box 1**. It is generally possible to acquire a high-quality diffusion dataset on a state-of-the-art clinical scanner in 5–30 min. The subject should be asked to lie as still as possible during the acquisition. Strongly motion-artifacted data should be discarded from the study.

Analysis of diffusion MRI data ● TIMING 1–5 h + 10 min per subject researcher time; 20–500 h computation time

4| Follow the procedure detailed in the TBSS manual (http://www.fmrib.ox.ac.uk/fsl/tbss) for a standard voxelwise cross-subject analysis using TBSS. First, correct the data for head motion and eddy currents using affine registration (and a correlation ratio or mutual information cost function). Then fit a diffusion tensor model to the set of diffusion-weighted images, from which at least the FA image is kept[9]. Run the FSL TBSS scripts (see **Box 2**). This results in a single 4D image, where the fourth dimension is subject ID. This is ready to be fed into voxelwise statistics, for example, testing at each skeleton

BOX 2 | RUNNING THE TRACT-BASED SPATIAL STATISTICS (TBSS) SCRIPTS

- Before running TBSS, eddy current and head motion effects should be corrected (e.g., using the FSL program **eddy_correct**) and then the tensor model, producing the FA image, should be fitted (e.g., using the FSL program **dtifit**).
- **Preprocessing** ensures that the FA data are in the right format. All FA images and their histograms should be checked visually at this stage for artifacts, intensity range problems and general data quality (**Fig. 1** shows a good-quality image and its histogram). If both tails of the histogram cannot be seen to fall cleanly to zero, there is probably an intensity range problem.
- **Registration and post-registration** applies non-linear registration directly to all subjects' FA images, transforming all data into a higher-resolution FA standard space. Next the mean FA across all subjects is created, and then the skeletonized mean FA image, onto which all FA data will ultimately be projected. All aligned FA images should be checked (e.g., as a 'cross-subject movie loop' underneath the thresholded mean FA skeleton) to ensure that all subjects' registrations gave reasonable output, that the skeleton is being thresholded at a suitable level and that each part of the thresholded skeleton is near a suitable tract in each subject. The threshold applied to the mean FA skeleton may need to be changed from the default, as a suitable threshold will depend on factors such as overall image quality and heterogeneity of subjects. The skeleton should be a good representation of the centers of the tracts that are consistent across subjects. If there is poor correspondence between the thresholded skeleton and the aligned FA data then either the registrations or the skeleton threshold level needs to be corrected (**Fig. 2** shows four example subjects after alignment, underneath the common mean FA skeleton).
- **Prestats** then projects all subjects' non-linearly aligned FA data onto the thresholded mean FA skeleton.

voxel where one group of subjects is different from another group. Skeleton-projected FA data have been shown to be Gaussian-distributed across subjects[12]; hence simple parametric statistics should result in valid voxelwise *P*-values (it has been shown[12,15] that FA is not distributed normally *before* skeleton-projection). However, correction for multiple comparisons (across voxels) is not straightforward; for example, random field theory[16] is likely to be inaccurate owing to variations in smoothness and local topology, including edge effects. Hence, we recommend generating corrected voxelwise or cluster-based *P*-values using permutation testing, generating the null distribution of the maximum (across space) test statistic[17]. For sample good-quality raw FA and skeleton images, see **Figures 1** and **2**, respectively.

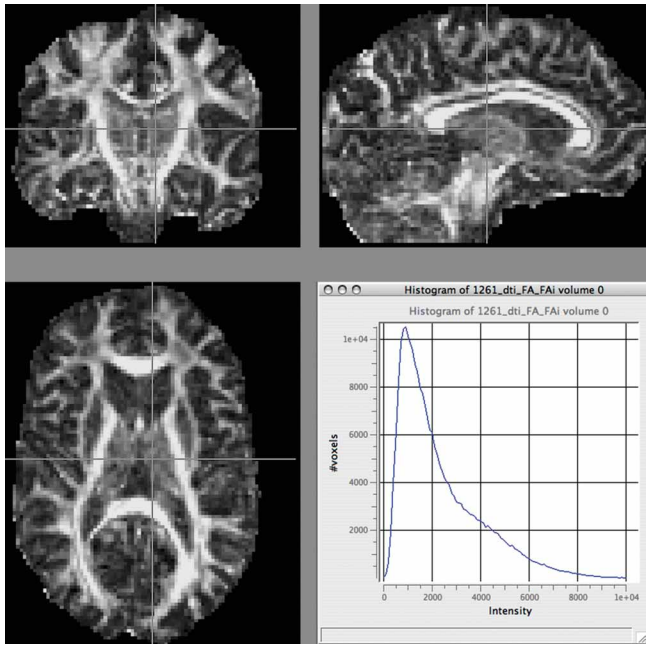

Figure 1 | Example good-quality fractional anisotropy image and its intensity histogram, after format conversion and rescaling of the original intensity range from 0:1 to 0:10,000. The resolution is 1.8 × 1.8 × 2 mm^3; the data were acquired at 3 T with 16 diffusion gradient directions and a *b* value of 1,000 s mm^{-2} (no repeats of $b = 0$ or diffusion-weighted images). The $b = 0$ image has a signal-to-noise ratio of approximately 25.

5| Investigate (optional) the other summary images derived from the diffusion tensor, particularly the three tensor eigenvalues (which describe the diffusion along the strongest, second-strongest orthogonal and weakest diffusion directions, respectively) and the mean diffusivity (the overall strength of diffusion). For example, as a reduction in FA may be due to a decrease in diffusion along the dominant tract direction (quantified, in general, by the principal eigenvalue) or an increase in diffusion perpendicular to tracts (shown by the second and/or third eigenvalues), it can be helpful when drawing biological conclusions to be able to make such distinctions through separate analyses of the different eigenvalues. For this purpose, use the non-linear warps, skeleton and skeleton-projection vectors derived from the main FA analysis to project the other diffusion-derived data onto the skeleton before applying cross-subject statistics on this data.

6| Further validate any findings using tractography in the areas of interest highlighted by TBSS (optional). Taking back (from the common space of the mean FA image) one or more tractography-seeding masks into each subject's native diffusion data space, and seeding probabilistic tractography, addresses the cross-subject correspondence problem in a way that is complementary to the approach of TBSS. Furthermore, explicit questions relating to remote connectivity can then be asked of the data (TBSS is restricted to looking at *localized* changes in diffusion characteristics).

● TIMING

Step 1, obtaining subjects' informed consent: 10 min per subject
Steps 2 and 3, MRI structural and diffusion data acquisition: 30–60 min per subject
Step 4, data preparation and visual quality checking per subject: 1–10 min; computation time depending on non-linear registration target chosen and number of subjects: approximately 20–500 h (can easily be parallelized across multiple computers); quality checking and running cross-subject statistics: 1–2 h (plus approximately 5 h computation time if permutation testing is used)

ANTICIPATED RESULTS

If there is a significant diffusion-related change that correlates with a relevant covariate across subjects (such as pathology or treatment group membership, disability level, illness duration, age), then one would expect this protocol to detect the change and localize it to the correct white matter areas. The typical cross-subject coefficient-of-variation in FA (in a homogeneous group of subjects) is 5–10% for skeleton voxels in the larger tracts and approximately 10–15% elsewhere[12]. This can be considered in the context of a typical effect; for example, aging (between the ages of 40 and 70 years) might reduce FA from 0.8 to 0.7 in the genu of the corpus callosum. **Figure 3** shows example results from a study of amyotrophic lateral sclerosis (a progressive neurodegenerative disease most prominently affecting the motor system).

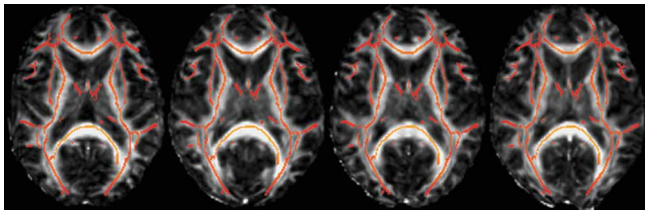

Figure 2 | Example mean fractional anisotropy (FA) skeleton (red-orange, thresholded at mean FA = 0.3), overlaid on four subjects' non-linearly registered FA images. The acquisition protocol was as for **Figure 1**.

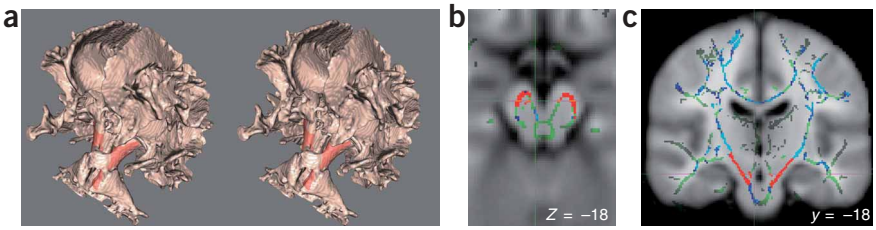

Figure 3 | Example results from a tract-based spatial statistics (TBSS) analysis of 13 amyotrophic lateral sclerosis (ALS) patients and 20 controls. (**a**) A 3D-rendered stereo pair of the mean fractional anisotropy (FA) skeleton. (**b,c**) Green shows mean FA skeleton, mostly hidden underneath blue and red. Blue shows where FA is significantly lower in ALS patients than in controls, after regressing out the effect of age. Red shows where FA correlates negatively with ALS progression rate in the ALS patients. The background image in (**b,c**) is the MNI152 standard space T1 template; the slice locations are in the MNI152 coordinate system. Reprinted from ref. 12 (2006) with permission from Elsevier; original data from O. Ciccarelli, Institute of Neurology, University College London.

ACKNOWLEDGMENTS The authors are supported by the UK Engineering and Physical Sciences Research Council, the Medical Research Council and the Wellcome Trust.

COMPETING INTERESTS STATEMENT The authors declare that the competing financial interests are too numerous to itemize.

Published online at http://www.natureprotocols.com
Reprints and permissions information is available online at http://npg.nature.com/reprintsandpermissions

1. Moseley, M.E. *et al.* Diffusion-weighted MR imaging of anisotropic water diffusion in cat central nervous system. *Radiology* **176**, 439–445 (1990).
2. Le Bihan, D. Looking into the functional architecture of the brain with diffusion MRI. *Nat. Rev. Neurosci.* **4**, 469–480 (2003).
3. Horsfield, M.A. & Jones, D.K. Application of diffusion-weighted and diffusion tensor MRI to white matter diseases—a review. *NMR Biomed.* **15**, 570–577 (2002).
4. Lim, K.O. & Helpern, J.A. Neuropsychiatric applications of DTI—a review. *NMR Biomed.* **15**, 587–593 (2002).
5. Moseley, M. Diffusion tensor imaging and aging—a review. *NMR Biomed.* **15**, 553–560 (2002).
6. Neil, J., Miller, J., Mukherjee, P. & Huppi, P.S. Diffusion tensor imaging of normal and injured developing human brain—a technical review. *NMR Biomed.* **15**, 543–552 (2002).
7. Buxton, R.B. Diffusion and the MR signal. In *Introduction to Functional Magnetic Resonance Imaging* 185–216 (Cambridge University Press, Cambridge, 2002).
8. Mori, S., Wakana, S., Nagae-Poetscher, L.M. & van Zijl, P.C.M. *MRI Atlas of Human White Matter.* Elsevier, Amsterdam, The Netherlands (2005).
9. Pierpaoli, C. & Basser, P.J. Toward a quantitive assessment of diffusion anisotropy. *Magn. Reson. Med.* **36**, 893–906 (1996).
10. Beaulieu, C. The basis of anisotropic water diffusion in the nervous system—a technical review. *NMR Biomed.* **15**, 435–455 (2002).
11. Ashburner, J. & Friston, K.J. Voxel-based morphometry—the methods. *NeuroImage* **11**, 805–821 (2000).
12. Smith, S.M. *et al.* Tract-based spatial statistics: voxelwise analysis of multi-subject diffusion data. *NeuroImage* **31**, 1487–1505 (2006).
13. Rueckert, D. *et al.* Nonrigid registration using free-form deformations: application to breast MR images. *IEEE Trans. Med. Imaging* **18**, 712–721 (1999).
14. Heiervang, E., Behrens, T.E., Mackay, C.E., Robson, M.D. & Johansen-Berg, H. Between session reproducibility and between subject variability of diffusion MR and tractography measures. *NeuroImage* **33**, 867–877 (2006).
15. Jones, D.K., Symms, M.R., Cercignani, M. & Howard, R.J. The effect of filter size on VBM analyses of DT-MRI data. *NeuroImage* **26**, 546–554 (2005).
16. Worsley, K.J. *et al.* A unified statistical approach for determining significant signals in images of cerebral activation. *Hum. Brain Mapp.* **4**, 58–73 (1996).
17. Nichols, T.E. & Holmes, A.P. Nonparametric permutation tests for functional neuroimaging: a primer with examples. *Hum. Brain Mapp.* **15**, 1–25 (2002).
18. Jones, D.K., Horsfield, M.A. & Simmons, A. Optimal strategies for measuring diffusion in anisotropic systems by magnetic resonance imaging. *Magn. Reson. Med.* **42**, 515–525 (1999).
19. Jones, D.K. The effect of gradient sampling schemes on measures derived from diffusion tensor MRI: a Monte Carlo study. *Magn. Reson. Med.* **51**, 807–815 (2004).
20. Behrens, T.E.J. *et al.* Characterization and propagation of uncertainty in diffusion-weighted MR imaging. *Magn. Reson. Med.* **50**, 1077–1088 (2003).
21. Gudbjartsson, H. & Patz, S. The Rician distribution of noisy MRI data. *Magn. Reson. Med.* **34**, 910–914 (1995).
22. Andersson, J.L.R., Skare, S. & Ashburner, J. How to correct susceptibility distortions in spin-echo echo-planar images: application to diffusion tensor imaging. *NeuroImage* **20**, 870–888 (2003).
23. Liu, C., Bammer, R., Kim, D.-H. & Moseley, M.E. Self-navigated interleaved spiral (SNAILS): application to high-resolution diffusion tensor imaging. *Magn. Reson. Med.* **52**, 1388–1396 (2004).
24. Pipe, J.G., Farthing, V.G. & Forbes, K.P. Multishot diffusion-weighted FSE using PROPELLER MRI. *Magn. Reson. Med.* **47**, 42–52 (2002).
25. Alexander, D.C. & Barker, G.J. Optimal imaging parameters for fiber-orientation estimation in diffusion MRI. *NeuroImage* **27**, 357–367 (2005).
26. Pierpaoli, C., Marenco, S., Rohde, G., Jones, D.K. & Barnett, A.S. Analyzing the contribution of cardiac pulsation to the variability of quantities derived from the diffusion tensor. *Proc. Intl. Soc. Mag. Reson. Med.* 70 (2003).
27. Pruessmann, K.P. Encoding and reconstruction in parallel MRI. *NMR Biomed.* **19**, 288–299 (2006).
28. Bammer, R. *et al.* Diffusion tensor imaging using single-shot SENSE-EPI. *Magn. Reson. Med.* **48**, 128–136 (2002).
29. Smith, S.M., Johansen-Berg, H., Mackay, C., Behrens, T.E. & Bartsch, A.J. Voxelwise analysis of FA data: session and subject variability, Gaussianity and dependence on acquisition. *Proc. Intl. Soc. Mag. Reson. Med.* 1063 (2006).

Erratum: Acquisition and voxelwise analysis of multi-subject diffusion data with Tract-Based Spatial Statistics

Stephen M Smith, Heidi Johansen-Berg, Mark Jenkinson, Daniel Rueckert, Thomas E Nichols, Karla L Miller, Matthew D Robson, Derek K Jones, Johannes C Klein, Andreas J Bartsch & Timothy E J Behrens

Nat. Protoc. doi:10.1038/nprot.2007.45; published online 15 March; corrected online 29 March 2007

In the version of this article originally published online, the URL given in EQUIPMENT SETUP, under "Computing equipment", should have been http://www.fmrib.ox.ac.uk/fsl. In the first line of **Box 2**, "head motion" should have read "head motion effects". In the legend to **Figure 1**, "and $a \cdot b$ value" should have been "and a b value" and "an signal-to-noise ratio" should have been "a signal-to-noise ratio". These errors have been corrected in all versions of the article.